

Adsorption and Corrosion Inhibition Characteristics of Some Thiophene-3-Carbohydrazide Derivatives on Low Carbon Steel in Hydrochloric Acid Solutions

Abd El-Aziz S. Fouda^{1*}, M. A. Diabb² and Doaa A. Badawya¹

¹Department of Chemistry, Faculty of Science, Mansoura University, Mansoura-35516, Egypt.

²Department of Chemistry, Faculty of Science, University of Damietta, Damietta 34517, Egypt.

Authors' contributions

This work was carried out in collaboration between all authors. All authors read and approved the final manuscript.

Article Information

DOI: 10.9734/IRJPAC/2015/17491

Editor(s):

(1) Wolfgang Linert, Institute of Applied Synthetic Chemistry Vienna University of Technology Getreidemarkt, Austria.

Reviewers:

(1) Anonymous, Jayaraj Annapackiam College for Women, India.

(2) Anonymous, Jamia Millia Islamia (Central University), India.

(3) Anonymous, University Mohamed 1st, Morocco.

(4) P. Krishnamoorthy, Department of Chemistry, Dr. Ambedkar Government Arts College, Chennai – 600 039, India.

Complete Peer review History: <http://www.sciencedomain.org/review-history.php?iid=1050&id=7&aid=9303>

Original Research Article

Received 16th March 2015
Accepted 1st April 2015
Published 19th May 2015

ABSTRACT

New compounds namely amino-N'-(3-(hydroxyimino)butan-2-ylidene)-4,5,6,7-tetrahydrobenzo[b]thiophene-3-carbohydrazide (1), amino-N'-(thiophen-2-ylmethylene)-4,5,6,7-tetrahydrobenzo[b]thiophene-3-carbohydrazide (2) and amino-N'-(1-(pyridin-2-yl)ethylidene)-4,5,6,7-tetrahydrobenzo[b]thiophene-3-carbohydrazide (3) were synthesized and used as corrosion inhibitors for carbon steel in 1 M hydrochloric acid at 25°C using different monitoring techniques. Potentiodynamic polarization studies showed that these derivatives were mixed type inhibitors. The effect of temperature on the corrosion behavior of carbon steel in 1 M HCl in presence and absence of these compounds at were studied. The adsorption of these inhibitors on carbon steel surface from hydrochloric acid obeyed the Langmuir adsorption isotherm. Quantum chemical method is used to explore the relationship between the inhibitors molecular properties and their inhibition efficiency.

Keywords: Corrosion inhibition; C- steel; HCl; thiophene 3-carbohydrazide derivatives EFM; EIS.

*Corresponding author: E-mail: asfouda@mans.edu.eg;

1. INTRODUCTION

Corrosion of materials cause's big losses in the economy of many countries due to the huge amount of funds needed in order to reduce it. Corrosion inhibition of metals, especially of steel, has received a lot of attention because of its widespread use in the industry such as the oil and gas [1], beverage, metallurgy among others, and thus, a lot of research in the field of corrosion inhibition of steel is necessary. Aqueous solutions of acids are among the most corrosive media and are widely used in industries for pickling, acid cleaning of boilers, descaling and oil well [2,3]. The main problem concerning C- steel applications is its relatively low corrosion resistance in acidic solution. Several methods used currently to reduce corrosion of C- steel. One of such methods is the use of organic inhibitors [4-7]. Effective inhibitors are heterocyclic compounds that have π bonds, heteroatoms such as sulphur, oxygen and nitrogen [8]. Compounds containing both nitrogen, sulphur and oxygen atoms can provide excellent inhibition, compared with compounds containing only two atoms from the three atoms [9]. Heterocyclic compounds such as thiophene 3-carbohydrazide derivatives can provide excellent inhibition. These molecules depend mainly on certain physical properties of the inhibitor molecules such as functional groups, steric factors, electron density at the donor atom and electronic structure of the molecules [10,11]. Many *N*-heterocyclic compounds have been used for the corrosion inhibition of metals, such as imidazoline [12], triazole [13-15], tetrazole [16], pyrrole [17], pyridine [18], pyrazole and bipyrazole [19,20], pyrimidine [21], pyridazine [22] and some derivatives. Some heterocyclic compounds containing a mercapto group have been developed as copper corrosion inhibitors. These compounds include: 2-mercaptobenzothiazole [23], 2,4-dimercapto pyrimidine [24], 2-amino-5-mercaptothiadzole, 2-mercaptothiazoline [25], potassium ethyl xanthate [26], indole and derivatives [27] and some thiophene derivatives [28-31]. Corrosion inhibition occurs through adsorption of organic compounds on the corroding metal surface following some known adsorption isotherms. The resulting adsorption film acts as a barrier that isolates the metal from the corroding and the efficiency of inhibition depends on the mechanical, structural and chemical

characteristics of the adsorption layer formed under particular conditions [32-36].

The purpose of this paper is to compare the corrosion inhibition data derived from EFM with that obtained from Tafel extrapolation and EIS techniques and to discuss the relationship between quantum chemical calculations and experimental protection efficiencies of the tested compounds.

2. EXPERIMENTAL DETAILS

2.1 Materials and Solutions

Experiments were performed using carbon steel specimens with composition (weight %): C 0.2, Mn 0.35, P 0.024, Si 0.003 and Fe is the rest. Hydrochloric acid (37%), ethyl alcohol and acetone were purchased from Al-Gomhoria Company, Egypt. Bidistilled water was used throughout all the experiments. These derivatives were synthesized as before [37] and their chemical structures are shown in Table 1.

2.2 Electrochemical Measurements

The experiments were carried out potentiodynamically in a thermostated three electrode cell. Platinum foil was used as counter electrode and a saturated calomel electrode (SCE) coupled to a fine Luggin capillary as the reference electrode. The working electrode was in the form of a square cut from C- steel under investigation and was embedded in a Teflon rod with an exposed area of 1 cm². This electrode was immersed in 100 ml of a test solution for 30 min until a steady state open-circuit potential (E_{ocp}) was attained. The potentiodynamic curves were recorded by changing the electrode potential from -1.0 to 0.0 V versus SCE with scan rate of 1 mVs⁻¹. All experiments were carried out in freshly prepared solution at constant temperature (25°C) using a thermostat. %IE and the degree of surface coverage (θ) were defined as:

$$\% IE = \theta \times 100 = [(i_{corr} - i_{corr(inh)}) / i_{corr}] \times 100 \quad (1)$$

where i_{corr} and $i_{corr(inh)}$ are the uninhibited and inhibited corrosion current density values, respectively, determined by extrapolation of Tafel lines.

Table 1. Molecular structures, formulas and molecular weights of the investigated thiophene 3-carbohydrazide derivatives

Comp.	Structures	Names	Chemical formulas	Molecular weights
1		amino-N'-(3-(hydroxyimino)butan-2-ylidene)-4,5,6,7-tetrahydrobenzo[b]thiophene-3-carbohydrazide	C ₁₃ H ₁₈ N ₄ O ₂ S	294.37
2		amino-N'-(thiophen-2-ylmethylene)-4,5,6,7-tetrahydrobenzo[b]thiophene-3-carbohydrazide	C ₁₄ H ₁₅ N ₃ OS ₂	305.42
3		amino-N'-(1-(pyridin-2-yl)ethylidene)-4,5,6,7-tetrahydrobenzo[b]thiophene-3-carbohydrazide	C ₁₆ H ₁₈ N ₄ OS	341.41

The electrochemical impedance spectroscopy (EIS) spectra were recorded at open circuit potential (OCP) after immersion the electrode for 30 min in the test solution. The ac signal was 5 mV peak to peak and the frequency range studied was between 100 kHz and 0.2 Hz.

The inhibition efficiency (% IE) and the surface coverage (θ) of the used inhibitors obtained from the impedance measurements were calculated by applying the following relations:

$$\% \text{ IE} = \theta \times 100 = [1 - (R_{ct}^{\circ} / R_{ct})] \quad (2)$$

Where, R_{ct}° and R_{ct} are the charge transfer resistance in the absence and presence of inhibitor, respectively.

EFM experiments were performed with applying potential perturbation signal with amplitude 10 mV with two sine waves of 2 and 5 Hz. The choice for the frequencies of 2 and 5 Hz was based on three arguments [38]. The larger peaks were used to calculate the corrosion current density (i_{corr}), the Tafel slopes (β_c and β_a) and the causality factors CF-2 and CF-3 [39].

All electrochemical experiments were carried out using Gamry instrument PCI300/4 Potentiostat/Galvanostat/Zra analyzer, DC105 Corrosion software, EIS300 Electrochemical impedance spectroscopy software, EFM140 electrochemical frequency modulation software and Echem Analyst 5.5 for results plotting, graphing, data fitting and calculating.

2.3 Theoretical Study

Accelrys (Material Studio Version 4.4) software for quantum chemical calculations has been used.

3. RESULTS AND DISCUSSION

3.1 Potentiodynamic Measurements

Polarization

Fig. 1 shows the potentiodynamic polarization curves for C- steel without and with different concentrations of compound (1) at 25°C. Similar curves for other compounds were obtained (not shown). The obtained electrochemical parameters; cathodic (β_c) and anodic (β_a) Tafel slopes, corrosion potential (E_{corr}), and corrosion current density (i_{corr}), were obtained and are listed in Table 2. Results of this Table show that i_{corr} decreases by adding the thiophene 3-carbohydrazide compounds and by increasing their concentrations. In addition, E_{corr} does not change obviously. Also β_a and β_c do not change markedly, which indicates that these compounds are mixed type inhibitors [40,41]. The parallel Tafel lines, indicate that there is no change in the mechanism of the corrosion reaction of C- steel. Fig. 1 clearly shows that both anodic and cathodic reactions are inhibited. The inhibition achieved by these compounds decreases in the following order: 3 > 2 > 1.

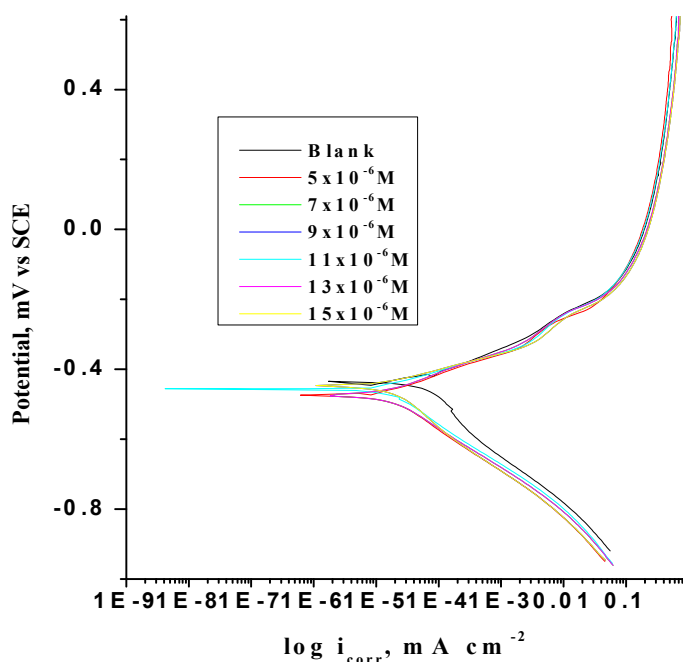


Fig. 1. Potentiodynamic polarization curves for the corrosion of C-steel in 2 M HCl in the absence and presence of various concentrations of compound (1) at 25°C

Table 2. Effect of concentrations of the investigated compounds on the free corrosion potential ($E_{corr.}$), corrosion current density ($i_{corr.}$), Tafel slopes (β_a & β_c), degree of surface coverage (θ) and inhibition efficiency (% IE) for C-steel in 2 M HCl at 25°C

Compounds	Conc., M	$-E_{corr.}$, mV(vs SCE)	i_{corr} , $\mu\text{A cm}^{-2}$	β_a , mV dec ⁻¹	β_c , mV dec ⁻¹	θ	% IE
(1)	Blank	480	19.91	101.5	148.5	----	-----
	5×10^{-6}	466	8.85	67.9	127.5	0.555	55.5
	7×10^{-6}	479	8.84	74.0	128.2	0.556	55.6
	9×10^{-6}	454	8.78	64.8	136.0	0.559	55.9
	11×10^{-6}	466	8.60	87.3	162.5	0.568	56.8
	13×10^{-6}	479	8.46	71.5	125.3	0.575	57.5
	15×10^{-6}	466	8.38	82.9	186.3	0.579	57.9
(2)	5×10^{-6}	466	8.25	81.7	184.3	0.587	58.7
	7×10^{-6}	466	8.15	87.7	196.0	0.591	59.1
	9×10^{-6}	466	8.00	87.3	162.5	0.598	59.8
	11×10^{-6}	466	7.87	80.4	187.7	0.605	60.5
	13×10^{-6}	466	7.54	64.4	125.3	0.621	62.1
	15×10^{-6}	477	6.70	84.2	132.5	0.663	66.3
(3)	5×10^{-6}	466	6.08	73.2	144.9	0.695	69.5
	7×10^{-6}	460	6.03	73.5	144.0	0.697	69.7
	9×10^{-6}	439	5.90	70.9	183.9	0.704	70.4
	11×10^{-6}	439	5.76	67.4	169.9	0.712	71.2
	13×10^{-6}	467	4.95	87.9	157.3	0.751	75.1
	15×10^{-6}	453	4.62	63.6	134.7	0.768	76.8

3.2 Adsorption Isotherms

The adsorption isotherms are considered to describe the interactions of the inhibitor molecule with the active sites on the metal surface [42]. Attempts were made to fit Θ values to various isotherms including Frumkin, Langmuir, Temkin, and Freundlich. The results were best fitted by far by the Langmuir adsorption isotherm (Fig.3) which has the following equation [29-30]:

$$C/\Theta = 1/K_{\text{ads}} + C \quad (3)$$

where C is the concentration of thiophene 3-carbohydrazide; K_{ads} is the adsorptive equilibrium constant; and Θ is the surface coverage of thiophene 3-carbohydrazide on C- steel, which can be calculated by the ratio of $IE/100$ for different thiophene 3-carbohydrazide concentration. Figs. 2 and 3 show the straight lines of C/Θ vs. C at T_1 (25°C) and T_2 (45°C), respectively.

Moreover, the adsorption heat can be calculated according to the van't Hoff equation [43]:

$$\ln K_{\text{ads}} = \Delta H_{\text{ads}}^0/RT + \text{const} \quad (4)$$

where ΔH^0 is the adsorption heat, R is the gas constant, T is the absolute temperature, K_1 and K_2 are the adsorptive equilibrium constants at T_1 (25°C) and T_2 (45°C), respectively. In consideration that the experiments proceed at the standard pressure and the solution concentrations are not very high, which are close to the standard condition, the calculated adsorption heat thus can be approximately regarded as the standard adsorption heat ΔH_{ads}^0 . The negative values of ΔH^0 Table 3 reflect the exothermic behavior of the adsorption of thiophene 3-carbohydrazide derivatives on the C-steel surface. The standard adsorption free energy (ΔG_{ads}^0) can be obtained according to the following equation [44,45].

$$K_{\text{ads}} = 1/55.5 \exp(-\Delta G_{\text{ads}}^0/RT) \quad (5)$$

The negative values of ΔG_{ads}^0 (Table 3) suggest that the adsorption of thiophene 3-carbohydrazide derivatives on the C- steel surface is spontaneous. Generally, the values of ΔG_{ads}^0 around or less than -20 kJ mol^{-1} are associated with the electrostatic interaction between charged molecules and the charged metal surface (physisorption); while those around or higher than -40 kJ mol^{-1} mean charge sharing or transfer from the inhibitor molecules to the metal surface to form a coordinate type of metal bond (chemisorption). The ΔG_{ads}^0 values listed in Table 3 are around -20 kJ mol^{-1} , which means that the adsorption of thiophene 3-carbohydrazide derivatives on the C-steel surface belongs to the physisorption and the adsorptive film has an electrostatic character [46, 47]. Finally, the standard adsorption entropy ΔS_{ads}^0 can be calculated by the following Eq:

$$\Delta S_{\text{ads}}^0 = (\Delta H_{\text{ads}}^0 - \Delta G_{\text{ads}}^0)/T \quad (6)$$

The (ΔS_{ads}^0) values (Table 3) are positive, which are opposite to the usual expectation that the adsorption is an exothermic process and always accompanied by a decrease of entropy. The reason can be explained as follows: the adsorption of thiophene 3-carbohydrazide inhibitor molecules from the aqueous solution can be regarded as a quasi-substitution process between the thiophene 3-carbohydrazide compound in the aqueous phase and water molecules at the electrode surface [$\text{H}_2\text{O}_{(\text{ads})}$] [48-51]. In this situation, the adsorption of thiophene 3-carbohydrazide derivatives is accompanied by the desorption of water molecules from the electrode surface. Thus, while the adsorption process for the inhibitor is believed to be exothermic and associated with a decrease in entropy of the solute, the opposite is true for the solvent [52]. The thermodynamic values obtained are the algebraic sum of the

Table 3. Some parameters from Langmuir isotherm model for C- steel in 2 M HCl for thiophene 3-carbohydrazide derivatives

Compounds	Temp., K	K_{ads} M^{-1}	$-\Delta G_{\text{ads}}^0$ kJ mol^{-1}	$-\Delta H_{\text{ads}}^0$ kJ mol^{-1}	ΔS_{ads}^0 $\text{J mol}^{-1}\text{k}^{-1}$
(1)	298	0.327	7.182	5.87	4.39
	318	0.396	7.657		
(2)	298	0.447	7.957	5.04	9.76
	318	0.473	8.097		
(3)	298	0.567	8.546	1.75	22.78
	318	0.570	8.559		

adsorption of thiophene 3-carbohydrazide inhibitor molecules and the desorption of water molecules. Therefore, the gain in entropy is attributed to the increase in solvent entropy. The positive values of (ΔS°_{ads}) suggest that the adsorption process is accompanied by an increase in entropy, which is the driving force for the adsorption of thiophene 3-carbohydrazide derivatives on the C-steel surface. Table 3 lists all the above calculated thermodynamic parameters.

3.2 Effect of Temperature

The importance of temperature variation in corrosion study involving the use of inhibitors is to determine the mode of inhibitor adsorption on

the metal surface. Recently, the use of two temperatures to establish the mode of inhibitor adsorption on a metal surface has been reported and has been found to be adequate [53,54]. Thus, the influence of temperature on the corrosion behavior of C- steel in 2 M HCl in the absence and presence of thiophene 3-carbohydrazide derivatives were investigated by polarization method at 25 and 45°C. Therefore, in examining the effect of temperature on the corrosion process, the apparent activation energies (E_a) were calculated from the Arrhenius equation [55]

$$\text{Log}(p_2/p_1) = (E_a/2.303R)(1/T_1 - 1/T_2) \quad (7)$$

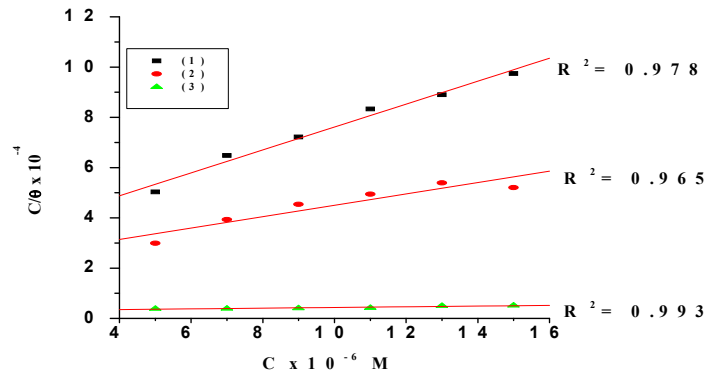


Fig. 2. Langmuir adsorption isotherm plotted as (C/θ) vs. C of thiophene 3-carbohydrazide derivatives for the corrosion of C- steel in 2 M HCl at 25°C

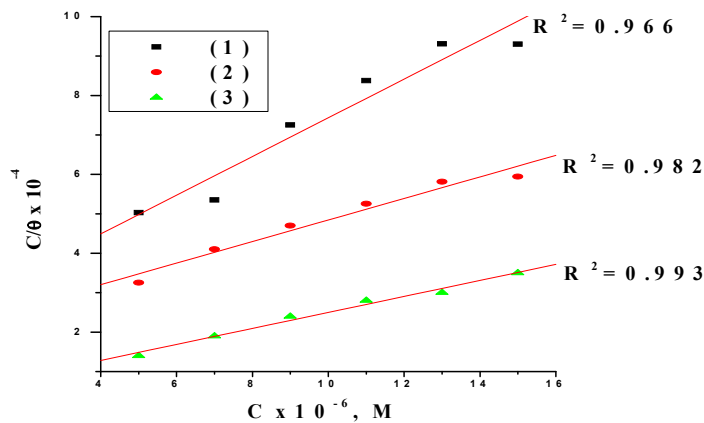


Fig. 3. Langmuir adsorption isotherm plotted as (C/θ) vs. C of thiophene 3-Carbohydrazide derivatives for the corrosion of C- steel in 2 M HCl at 45°C

where ρ_2 and ρ_1 are the corrosion rates at temperature T_1 and T_2 respectively. An estimate of heat of adsorption was obtained from the trend of surface coverage with temperature as follows [45]:

$$Q_{\text{ads}} = 2.303R [\log (\theta_2/1-\theta_2) - \log (\theta_1/1-\theta_1)] \times (T_1 \times T_2 / T_1 - T_2) \text{ kJ mol}^{-1} \quad (8)$$

where θ_1 and θ_2 are the degrees of surface coverage at temperatures T_1 and T_2 . The calculated values for both parameters are given in Table 4. Increased activation energy (E_a) in inhibited solutions compared to the blank suggests that the inhibitor is physically adsorbed on the corroding metal surface. It is seen from Table 4 that E_a values were higher in the presence of the additives compared to that in their absence hence leading to reduction in the corrosion rates. It has been suggested that adsorption of an organic inhibitor can affect the corrosion rate by either decreasing the available reaction area (geometric blocking effect) or by modifying the activation energy of the anodic or cathodic reactions occurring in the inhibitor-free surface in the course of the inhibited corrosion process [56]. The E_a values support the earlier proposed physisorption mechanism. Hence, corrosion inhibition is assumed to occur primarily through physical adsorption on the C- steel surface, giving rise to the deactivation of these surfaces to hydrogen atom recombination. Similar results have been reported in earlier

publications [57]. The negative Q_{ads} values indicate that the degree of surface coverage decreased with rise in temperature, supporting the earlier proposed physisorption mechanism [58].

3.2 Electrochemical Impedance Spectroscopy (EIS) Measurements

The corrosion of C- steel in 2 M HCl in the presence of the investigated compounds was investigated by EIS method at 25°C after 30 min immersion. Nyquist plots in the absence and presence of investigated compound (1) is presented in Fig. 4. Similar curves were obtained for other inhibitors but not shown. It is apparent that all Nyquist plots show a single capacitive loop, both in uninhibited and inhibited solutions. The impedance data of C- steel in 2 M HCl are analyzed in terms of an equivalent circuit model Fig. 5 which includes the solution resistance R_s and the double layer capacitance C_{dl} which is placed in parallel to the charge transfer resistance R_{ct} [59] due to the charge transfer reaction. For the Nyquist plots it is obvious that low frequency data are on the right side of the plot and higher frequency data are on the left. This is true for EIS data where impedance usually falls as frequency rises (this is not true for all circuits). The capacity of double layer (C_{dl}) can be calculated from the following equation:

$$C_{dl} = 1/2\pi f_{\text{max}} R_{ct} \quad (9)$$

Table 4. Calculated values of activation energy (E_a^*) and heat of adsorption (Q_{ads}) for C- steel in 2 M HCl solutions containing various concentrations of thiophene 3-carbohydrazide derivatives at 25 and 45°C obtained from potentiodynamic polarization measurements

	Conc., M	E_a^* , kJ mol ⁻¹	- Q_{ads} , kJ mol ⁻¹
Blank	-----	1.8	-----
(1)	5×10^{-6}	2.4	1.0
	7×10^{-6}	2.9	1.6
	9×10^{-6}	3.2	1.8
	11×10^{-6}	3.5	2.4
	13×10^{-6}	3.6	2.9
	15×10^{-6}	3.7	3.1
(2)	5×10^{-6}	3.1	2.0
	7×10^{-6}	3.2	2.1
	9×10^{-6}	3.4	2.5
	11×10^{-6}	3.6	2.6
	13×10^{-6}	4.3	3.2
	15×10^{-6}	6.9	10.0
(3)	5×10^{-6}	5.3	3.0
	7×10^{-6}	5.8	3.7
	9×10^{-6}	6.2	4.5
	11×10^{-6}	6.3	4.9
	13×10^{-6}	8.4	10.1
	15×10^{-6}	10.0	10.4

where f_{max} is maximum frequency. The parameters obtained from impedance measurements are given in Table 5. It can be seen from Table 5 that the values of charge transfer resistance R_{ct} increase with inhibitor concentration [60]. In the case of impedance studies, % IE increases with inhibitor concentration in the presence of investigated inhibitors and the % IE of these investigated inhibitors is as follows: (3) > (2) > (1).

The impedance study confirms the inhibiting characters of these compounds obtained from

potentiodynamic polarization. It is also noted that the C_{dl} values tend to decrease when the concentration of these compounds increases. This decrease in C_{dl} , which can result from a decrease in local dielectric constant and/or an increase in the thickness of the electrical double layer, suggests that these compounds function by adsorption at the metal/solution interface [61]. The inhibiting effect of these compounds can be attributed to their parallel adsorption at the metal solution interface. The parallel adsorption is owing to the presence of one or more active center for adsorption.

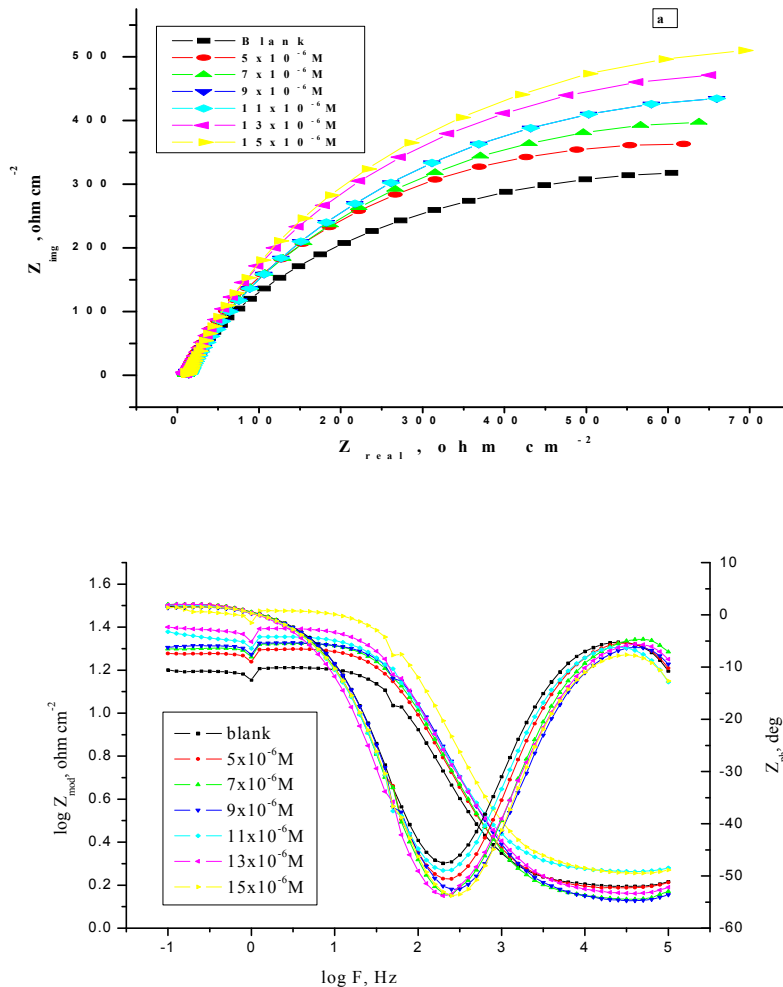


Fig. 4. The Nyquist (a) and Bode (b) plots for corrosion of C-steel in 2 M HCl in the absence and presence of different concentrations of compound (1) at 25°C

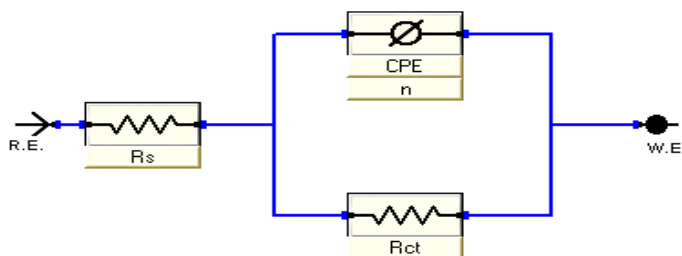


Fig. 5. Equivalent circuit model used to fit the impedance spectra

3.3 Electrochemical Frequency Modulation (EFM) Measurements

EFM is a nondestructive corrosion measurement technique that can directly and quickly determine the corrosion current value without prior knowledge of Tafel slopes, and with only a small polarizing signal. These advantages of EFM technique make it an ideal candidate for online corrosion monitoring [62]. The great strength of the EFM is the causality factors which serve as an internal check on the validity of EFM measurement. The causality factors CF-2 and CF-3 are calculated from the frequency spectrum of the current responses. Figs 6 shows the frequency spectrum of the current response of C-steel in 2 M HCl, contains not only the input frequencies, but also contains frequency components which are the sum, difference, and multiples of the two input frequencies. The EFM intermodulation spectrums of C- steel in 2 M HCl acid solution containing (15×10^{-6} M) of the studied compound (1) are shown in Fig 6. Similar results were recorded for the other concentrations of the investigated compounds (not shown). The harmonic and intermodulation peaks are clearly visible and are much larger than the background noise. The two large peaks, with amplitude of about 200 μ A, are the response to the 40 and 100 mHz (2 and 5 Hz) excitation frequencies. It is important to note that between the peaks there is nearly no current response (<100 nA). The experimental EFM data were treated using two different models: complete diffusion control of the cathodic reaction and the "activation" model. For the latter, a set of three non-linear equations had been solved, assuming that the corrosion potential does not change due to the polarization of the working electrode [63]. The larger peaks were used to calculate the corrosion current density (i_{corr}), the Tafel slopes (β_c and β_a) and the causality factors (CF-2 and CF-3). These electrochemical parameters were simultaneously determined by Gamry EFM140

software, and listed in Table 6. The data presented in Table 6 obviously show that, the addition of any one of tested compounds at a given concentration to the acidic solution decreases the corrosion current density, indicating that these compounds inhibit the corrosion of C- steel in 2 M HCl through adsorption. The causality factors obtained under different experimental conditions are approximately equal to the theoretical values (2 and 3) indicating that the measured data are verified and of good quality [64]. The inhibition efficiencies % I_{EFM} increase by increasing the studied inhibitors concentrations was calculated as follows:

$$\%I_{\text{EFM}} = [(1 - i_{\text{corr}} / i_{\text{corr}}^0)] \times 100 \quad (10)$$

Where i_{corr}^0 and i_{corr} are corrosion current densities in the absence and presence of inhibitor, respectively. The inhibition sufficiency obtained from this method is in the order: (3) > (2) > (1).

3.4 Quantum Chemical Calculations

Theoretical calculations were performed for only the neutral forms, in order to give further insight into the experimental results. Values of quantum chemical indices such as energies of LUMO and HOMO (E_{HOMO} and E_{LUMO}), the formation heat ΔH_f and energy gap ΔE , are calculated by semi-empirical PM3 methods has been given in Table 7. The reactive ability of the inhibitor is related to E_{HOMO} , E_{LUMO} [65]. Higher E_{HOMO} of the adsorbent leads to higher electron donating ability [66]. Low E_{LUMO} indicates that the acceptor accepts electrons easily. The calculated quantum chemical indices (E_{HOMO} , E_{LUMO} , μ) of investigated compounds are shown in Table 7. The difference $\Delta E = E_{\text{LUMO}} - E_{\text{HOMO}}$ is the energy required to move an electron from HOMO to LUMO. Low ΔE facilitates adsorption of the molecule and thus will cause higher inhibition

efficiency. The energy gap ΔE decreases as follows: (3 > 2 > 1). This fact explains the decreasing inhibition efficiency in this order (3 > 2 > 1, as shown in Table 7. Fig. 7 shows the optimized structures of the three investigated compounds. So, the calculated energy gaps

show reasonably good correlation with the efficiency of corrosion inhibition. Table (7) also indicates that compound (3) possesses the lowest total energy and higher dipole moment that means that compound (3) adsorption occurs easily and is favored by the highest softness.

Table 5. Electrochemical kinetic parameters obtained from EIS technique for the corrosion of C-steel in 2 M HCl at different concentrations of investigated inhibitors at 25°C

Comp.	Conc.,M.	$R_s, \Omega \text{cm}^2$	$Y_{oi}, x 10^{-3} \mu\Omega^{-1} \text{s}^n$	n	$R_{ct}, \Omega \text{cm}^2$	$C_{dl}, x 10^{-2} \mu\text{Fcm}^{-2}$	θ	%IE
	Blank	13.30	169.9	746.7	1.047	80.79	-----	-----
(1)	5×10^{-6}	13.28	169.5	743.8	1.256	80.19	0.625	62.5
	7×10^{-6}	13.29	169.4	743.6	1.258	80.06	0.626	62.6
	9×10^{-6}	10.92	157.1	777.2	1.328	75.82	0.646	64.6
	11×10^{-6}	10.65	171.5	769.8	1.330	75.22	0.647	64.7
	13×10^{-6}	10.65	171.4	769.6	1.331	75.66	0.647	64.7
	15×10^{-6}	10.92	123.1	742.7	1.367	73.65	0.656	65.6
(2)	5×10^{-6}	10.39	122.9	742.9	1.369	73.60	0.657	65.7
	7×10^{-6}	5.992	157.6	769.4	1.375	73.23	0.658	65.8
	9×10^{-6}	9.183	136.3	760.0	1.465	68.73	0.679	67.9
	11×10^{-6}	9.175	136.5	759.9	1.466	68.69	0.679	67.9
	13×10^{-6}	10.11	126.7	764.2	1.476	68.21	0.682	68.2
	15×10^{-6}	10.10	126.7	764.2	1.477	68.16	0.682	68.2
(3)	5×10^{-6}	10.51	166.8	758.3	1.542	65.32	0.695	69.5
	7×10^{-6}	11.35	157.3	769.7	1.556	64.72	0.698	69.8
	9×10^{-6}	11.35	157.4	769.6	1.558	64.64	0.698	69.8
	11×10^{-6}	9.876	163.7	767.1	1.736	58.02	0.729	72.9
	13×10^{-6}	15.16	152.9	772.0	1.879	53.61	0.749	74.9
	15×10^{-6}	15.17	153.0	773.0	1.880	53.58	0.750	75

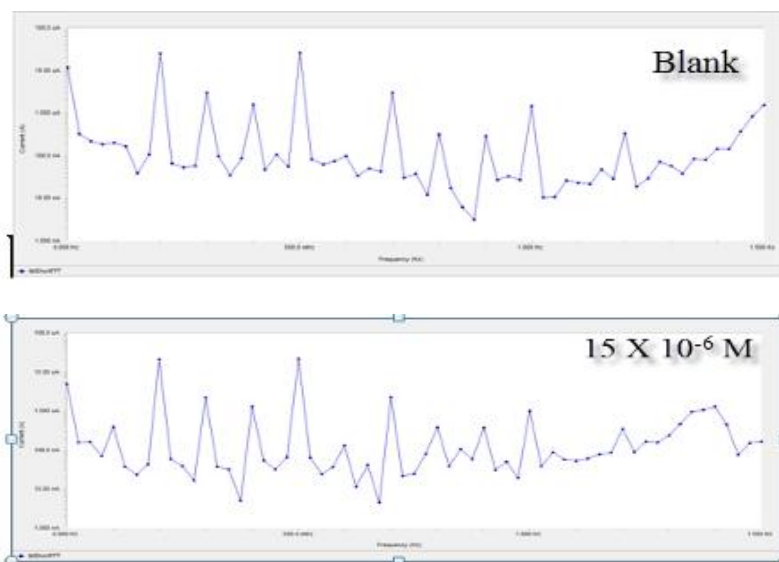


Fig. 6. EFM spectra C- steel in 2M HCl in the absence and presence of different concentrations of compound (1) at 25°C

Table 6. Electrochemical kinetic parameters obtained from EFM technique for the corrosion of C- steel in 2 M HCl at different concentrations of investigated inhibitors at 25°C

Comp.	Conc., M	i_{corr} , $\mu A\ cm^{-2}$	β_a , $mVdec^{-1}$	β_c , $mVdec^{-1}$	CF-2	CF-3	CR mpy	θ	% IE
	Blank	52.24	96	127	1.97	3.45	26.16	-	-
(1)	5×10^{-6}	40.10	85	108	1.93	2.92	22.30	0.232	23.2
	7×10^{-6}	38.66	111	198	1.89	2.38	17.71	0.259	25.9
	9×10^{-6}	36.68	106	190	1.93	3.27	16.76	0.294	29.4
	11×10^{-6}	35.36	92	189	2.07	3.06	16.16	0.323	32.3
	13×10^{-6}	33.62	104	126	1.77	3.74	15.36	0.356	35.6
	15×10^{-6}	32.86	76	147	1.95	2.50	15.02	0.379	37.9
(2)	5×10^{-6}	32.44	90	191	2.02	2.95	14.83	0.371	73.1
	7×10^{-6}	31.77	111	198	1.89	2.89	13.47	0.391	39.1
	9×10^{-6}	29.10	79	90	2.41	2.89	13.33	0.442	44.2
	11×10^{-6}	27.71	91	195	1.93	2.41	12.66	0.469	46.9
	13×10^{-6}	26.73	84	160	1.82	3.60	12.21	0.488	48.8
	15×10^{-6}	26.65	92	165	1.92	2.76	12.31	0.489	48.9
(3)	5×10^{-6}	22.05	87	152	1.92	3.18	10.50	0.577	57.7
	7×10^{-6}	19.22	83	129	1.87	2.81	8.78	0.632	63.2
	9×10^{-6}	17.23	87	146	1.83	2.95	6.95	0.670	67.0
	11×10^{-6}	17.20	46	148	1.89	3.19	5.36	0.671	67.1
	13×10^{-6}	16.89	73	145	1.85	3.17	6.80	0.676	67.6
	15×10^{-6}	15.53	53	168	2.17	2.62	4.35	0.702	70.2

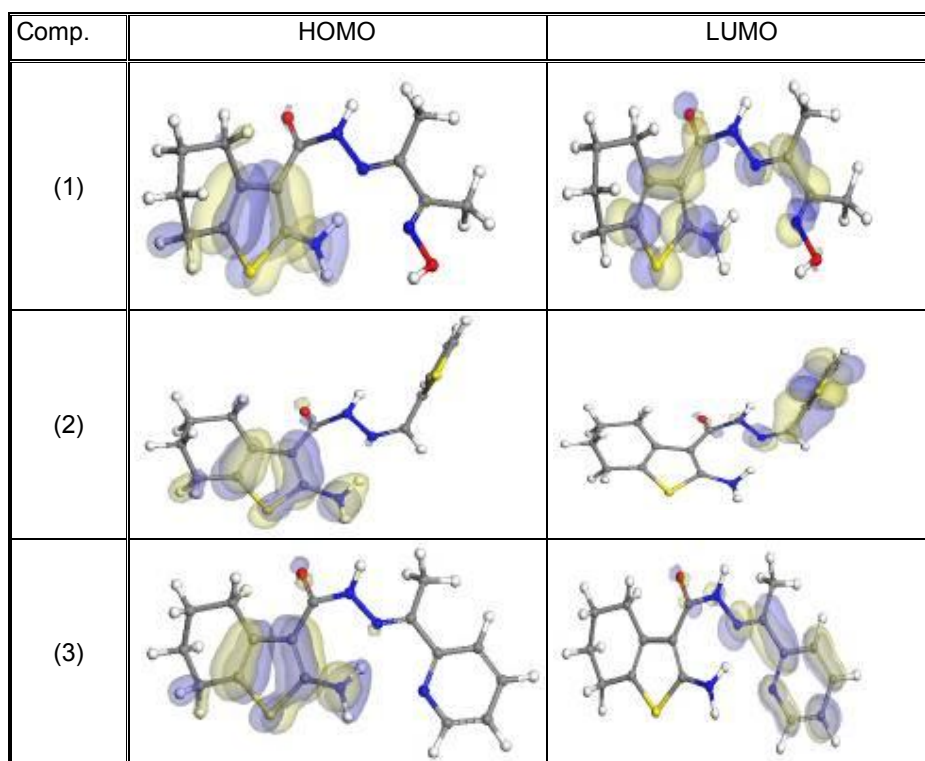
**Fig. 7. Molecular orbital plots of organic compounds**

Table 7. The calculated quantum chemical properties for investigated compounds

Parameters	(1)	(2)	(3)
-E _{HOMO} (eV)	8.538	8.501	8.248
-E _{LUMO} (eV)	0.192	0.868	0.898
ΔE (eV)	8.346	7.633	7.350
Dipole moment (Debye)	3.424	3.794	5.670

3.5 Chemical Structure of the Inhibitors and Corrosion Inhibition

Inhibition of the corrosion of C-steel in 2 M HCl solution by some thiophene 3-carbohydrazide derivatives is determined by potentiodynamic polarization and other methods, it was found that the inhibition efficiency depends on concentration, nature of metal, the mode of adsorption of the inhibitors and surface conditions. The observed corrosion data in presence of these inhibitors, namely: i) The decrease of corrosion rate and corrosion current with increase in concentration of the inhibitor ii) The linear variation of weight loss with time iii) The shift in Tafel lines to higher and lower potential regions iv) The decrease in corrosion inhibition with increasing temperature indicates that desorption of the adsorbed inhibitor molecules takes place and v) The inhibition efficiency was shown to depend on the number of adsorption active centers in the molecule and their charge densities. Polar character of substituents in the changing part of the inhibitor molecule seems to have a prominent effect on the electron charge density of the molecule. Metals such as Cu and Fe, which have a greater affinity towards aromatic moieties, were found to adsorb benzene rings in a flat orientation. The order of decreasing the inhibition efficiency of the investigated compounds in the corrosive solution was as follows: (3) > (2) > (1).

It is well known that the steel surface bears positive charge in acid solution [67], so it is difficult for the protonated molecules to approach the positively charged carbon steel surface due to the electrostatic repulsion. Since chloride ions have a smaller degree of hydration, thus they could bring excess negative charges in the vicinity of the interface and favor more adsorption of the positively charged inhibitor molecules, the protonated thiophene 3-carbohydrazide derivatives adsorb through electrostatic interactions between the positively charged

molecules and the negatively charged metal surface. Thus there is a synergism between adsorbed Cl⁻ ions and protonated thiophene 3-carbohydrazide derivatives. Thus we can conclude that inhibition of carbon steel corrosion in 2 M HCl is mainly due to electrostatic interaction. The decrease in inhibition efficiency with rise in temperature supports electrostatic interaction. In the second mode, since it is well known that the steel surface bears positive charge in acid solution [53, 54], so it is difficult for the protonated molecules to approach the positively charged carbon steel surface due to the electrostatic repulsion. Since chloride ions have a smaller degree of hydration, thus they could bring excess negative charges in the vicinity of the interface and favor more adsorption of the positively charged inhibitor molecules, the protonated thiophene azodyes adsorb through electrostatic interactions between the positively charged molecules and the negatively charged metal surface. Thus there is a synergism between adsorbed Cl⁻ ions and protonated thiophene azodyes. Thus we can conclude that inhibition of carbon steel corrosion in 2 M HCl is mainly due to electrostatic interaction. The decrease in inhibition efficiency with rise in temperature supports electrostatic interaction.

4. CONCLUSION

The tested thiophene 3-carbohydrazide derivatives establish a very good inhibition for C-steel corrosion in HCl solution. Thiophene 3-carbohydrazide derivatives inhibit C- steel corrosion by adsorption on its surface and act better than the passive oxide film. The inhibition efficiency is in accordance to the order: (3) > (2) > (1). The inhibition efficiencies of the tested compounds increase with increasing of their concentrations. Double layer capacitances decrease with respect to blank solution when the inhibitor added. This fact may explained by adsorption of the inhibitor molecule on the C-steel surface. The adsorption of these compounds on carbon steel surface in HCl solution follows Langmuir adsorption isotherm. The values of inhibition efficiencies obtained from the different independent techniques showed the validity of the obtained results.

COMPETING INTERESTS

Authors have declared that no competing interests exist.

REFERENCES

- Deyab MA. Inhibitive performance of glycolic acid ethoxylate 4-nonylphenyl ether in acid solution for corrosion of mild Steel. *Corros. Sci.* 2007;49:2315-2328.
- Abd El-Maksoud SA, Fouda AS. Investigation of Benzimidazole Compound as a Novel Corrosion Inhibitor for Mild Steel in Hydrochloric Acid Solution. *Mater. Chem. Phys.* 2005;93:84-90.
- Khaled KF, Mater. Thiophene derivatives as corrosion inhibitors for carbon steel in hydrochloric acid solutions. *Mater. Chem. Phys.* 2008;122:290-300.
- Avci G. Colloids Surf, Corrosion inhibition of carbon steel xc70 in h2so4 solution by ferrocene derivative 3-(ferrocenyl methylamine) benzonitrile, *J. Fundamental appl. Sci. A.* 2008;317:730-736.
- Pillali KC, Narayan R. New eco-friendly corrosion inhibitors based on phenolic derivatives for protection mild steel corrosion. *Corros. Sci.* 1985;23:151.
- Tadros AB, Abdel-Naby BA, *J. Electroanal. Chem.* 1988;224:433.
- Bockris JO'M, Yang B. Effect of New Synthesised Pyridazine Derivatives on the electrochemical behaviour of mild Steel in 1M HCl Solution. *J. Electrochem. Soc.* 1991;138:2237.
- Khalifa MA, El-Batouti M, Mhgoub F, Bakr Aknish A. *Corrps.* 2003;54:251-258.
- Abboud Y, Abourriche A. Saffag T, Berrada M, Charrouf M, Bennamara A, Al Himidi N, Hannache H. 2,3-Quinoxalinedione as a novel corrosion inhibitor for mild steel in 1 M HCl. *Mater. Chem. Phys.* 2007;105:1-5.
- Khaled KF. Electrochim, on the corrosion inhibition of iron in hydrochloric acid solutions, Part I: Electrochemical DC and AC studies. *Electrochim. Acta.* 2003;48: 2493-2503.
- Popova A, Chistov M, Raicheva S, Sokolova E. Quinazolin derivatives as eco-friendly corrosion inhibitors for low carbon steel in 2 M HCl solutions. *Corros. Sci.* 2004;46:1333-1350.
- Cruz J, Mart'inez R, Genesca J, Garc'ia-Ochoa E. Experimental and theoretical study of 1-(2-ethylamino)-2-methylimidazole as an inhibitor of carbon steel corrosion in acid media. *J. Electroanal. Chem.* 2004;566(1):111-121.
- Abdennabi AMS, Abdulhadi AI, Abu-Orabi ST, Saricimen H. The inhibition action of 1(benzyl)-1-H-4,5-dibenzoyl-1,2,3-triazole on mild steel in hydrochloric acid media. *Corros. Sci.* 1996;38(10):1791-1800.
- Bentiss F, Traisnel M, Gengembre L, Lagrenee M. New triazole derivative as inhibitor of the acid corrosion of mild steel: electrochemical studies, weight loss determination, SEM and XPS. *Appl. Surf. Sci.* 1999;152(3):237-249.
- Wang L. Inhibition of mild steel corrosion in phosphoric acid solution by triazole derivatives. *Corros. Sci.* 2006;48(3):608-616.
- Kertit S, Hammouti B. Corrosion inhibition of iron in 1M HCl by 1-phenyl-5-mercapto-1,2,3,4-tetrazole. *Appl. Surf. Sci.* 1996; 93(1):59-66.
- Hudson RM, Butler TJ, Warning CJ. The effect of pyrrole-halide mixtures in inhibiting the dissolution of low-carbon steel in sulphuric acid. *Corros. Sci.* 1977;17(7):571-581.
- Veloz MA, Mart'inez IG. Effect of some pyridine derivatives on the corrosion behavior of carbon steel in an environment like NAGE TM0177. *Corrosion.* 2006;62(4): 283-292.
- Ouchrif A, Zegmout M, Hammouti B, El-Kadiri S, Ramdani A. 1,3-Bis(3-hydroxymethyl-5-methyl-1-pyrazole) propane as corrosion inhibitor for steel in 0.5 M H2SO4 solution. *Appl. Surf. Sci.* 2005;252(2):339-344.
- Chetouani A, Hammouti B, Benhadda T, Daoudi M. Inhibitive action of bipyrazolic type organic compounds towards corrosion of pure iron in acidic media. *Appl. Surf. Sci.* 2005;249(1-4):375-385.
- Abd El-Maksoud SA. the influence of some arylazobenzoyl acetonitrile derivatives on the behaviour of carbon steel in acidic media. *Appl. Surf. Sci.* 2003;206(1-4):129-136.
- Chetouani A, Aouniti A, Hammouti B, Benchat N, Benhadda T, Kertit S, Corrosion inhibitors for iron in hydrochloride acid solution by newly synthesised pyridazine derivatives. *Corros. Sci.* 2003;45(8):1675-1684.
- Ohsawa M, Su'etaka W. Spectro-electrochemical studies of the corrosion inhibition of copper by mercapto-benzothiazole. *Corros. Sci.* 1979;19(7): 709-722.
- Walter GW. A review of impedance plot methods used for corrosion performance

- analysis of painted metals. *Corros. Sci.* 1986;26(9):681-703.
25. Trachli B, Keddami M, Takenouti H, Srhiri A. Protective effect of electropolymerized 3-amino 1,2,4-triazole towards corrosion of copper in 0.5M NaCl. *Corros. Sci.* 2002; 44(5):997–1008.
 26. Soriaga MP, Stickney J, Bottomley LA, Kim YG, Kluwer Eds. Academic/Plenum Publishers, New York, NY, USA; 2001.
 27. Hepel M, Scendo M. Kinetics of CuEtX film formation on copper piezoelectrodes. *J. Electroanal. Chem.* 2002;538-539:121–132.
 28. Scendo M. Potassium ethyl xanthate as corrosion inhibitor for copper in acidic chloride solutions. *Corros. Sci.* 2005;47(7): 1738–1749.
 29. Bishir Usman, Hasmerya Maarof, Hassan H. Abdallah, Rosmahaida Jamaludin, Abdo M. Al-Fakih, Madzlan Aziz, Corrosion inhibition efficiency of thiophene derivatives on mild steel: A QSAR model. *Int. J. Electrochem. Sci.* 2014;9:1678–1689.
 30. Inhibition of copper in HNO₃ solution using thiophene and its derivatives, *Arabian Journal of Chemistry*; 2011. in press.
 31. Sharfawati Che Soh, Madzlan Aziz Andrita Sundari. Polarization behavior of carbon steel corrosion in strong acid media in the presence of methyl thiophene inhibitor. *Ind. J. Sci. Res. Technol.* 2014;2(2):25-30.
 32. *Advances in Water Treatment by Adsorption Technology*, Nature London. 2006;1:2661-2667.
 33. The Quest for Active Carbon Adsorbent Substitutes: Inexpensive Adsorbents for Toxic Metal Ions Removal from Wastewater. *Sepr. & Purfn. Rev.* 2010;39: 95-171.
 34. New generation adsorbents for water treatment. *Chem. Revs.* 2012;112:5073-5091.
 35. Low cost adsorbents for removal of organic pollutants from wastewater. *J. Environ. Manag.* 2012;113:170-183.
 36. Water treatment by adsorption columns: Evaluation at ground level. *Sepr. & Purfn. Rev.* 2014;43(3):175-205.
 37. Matheus ME, Oliveira LF, Freitas AC, Carvalho AM, Barreiro AJ. *J. Med. Biol.* 1991;24:1219–1222.
 38. Bosch RW, Hubrecht J, Bogaerts WF, Syrett BC. Electrochemical frequency modulation: A new electrochemical technique for online corrosion monitoring. *J. Sci. Eng.* 2001;57:60-70.
 39. Abdel-Rehim SS, Khaled KF, Abd-Elshafi NS. Electrochemical frequency modulation as a new technique for monitoring corrosion inhibition of iron in acid media by new thiourea derivative. *Electrochim. Acta.* 2006;51:3269.
 40. Stupnisek-Lisac E, Gazivoda A, Madzarac M. 2-Mercapto-1-methylimidazole as corrosion inhibitor for copper in hydrochloric acid. *Electrochim. Acta.* 2002; 47:4189.
 41. Mu GN XHL, Quand Q, Zhou J, *Corros.Sci.* 2006;48:445.
 42. Sinyashin. The inhibition action of ammonium salts of O,O'-dialkyldithiophosphoric acid on carbon dioxide corrosion of mild steel. *Corros. Sci.* 2011;53:976.
 43. Torres VV, Amado RS, de Sá CF, Fernandez TL, Da Silva Riehl CA, Torres AG, D'Elia E. Inhibitory action of aqueous coffee ground extracts on the corrosion of carbon steel in HCl solution. *J. Corros. Sci.* 2011;53:2385.
 44. Zhao TP, Mu GN. The adsorption and corrosion inhibition of anion surfactants on aluminium surface in hydrochloric acid. *Corros. Sci.* 1999;41:1937.
 45. Bahrami MJ, Hosseini SMA, Pilvar P. Experimental and theoretical investigation of organic compounds as inhibitors for mild steel corrosion in sulfuric acid medium. *Corros. Sci.* 2010;52:2793.
 46. Obot IB, Obi-Egbed NO. An interesting and efficient green corrosion inhibitor for aluminium from extracts of *Chlomolaena odorata* L. in acidic solution. *J. Appl. Electrochem.* 2010;40:1977–1984.
 47. Ostovari A, Hoseinieh SM, Peikari M, Shadizadeh SR, Hashemi SJ. Corrosion inhibition of mild steel in 1 M HCl solution by henna extract: A comparative study of the inhibition by henna and its constituents (Lawsone, Gallic acid, α-d-Glucose and Tannic acid). *Corros. Sci.* 2009;51:1935–1949.
 48. Bouklah M, Hammouti B, Lagrenée M, Bentiss F. Thermodynamic properties of 2,5-bis(4-methoxyphenyl)-1,3,4-oxadiazole as a corrosion inhibitor for mild steel in normal sulfuric acid medium. *Corros. Sci.* 2006;48:2831.
 49. Donahue FM, Nobe K. *J. Electrochem. Soc.* 1965;112:886.

50. Kamis E, Bellucci F, Latanision RM, El-Ashry ESH. Corrosion. 1991;47:677.
51. Li XH, Deng SD, Fu H, Mu GN. Synergistic inhibition effect of rare earth cerium(IV) ion and sodium oleate on the corrosion of cold rolled steel in phosphoric acid solution. Corros. Sci. 2010;52:1167.
52. Gomma GK, Wahdan MH. Mater. Chem. Phys. 1995;39.
53. Marsh J. Advanced Organic Chemistry, 3rd ed., Wiley Eastern New Delhi; 1988.
54. Soliman MS. Ph. D. Thesis, Alex. Univ., Egypt; 1995.
55. Abdallah M. Tetrahydrocarbazole Derivatives as Corrosion inhibitors for zinc in HCl solution. Corros. Sci. 2003;45:2705.
56. Fouda AS, Al-Sarawy AA, El-Katori EE. Desalination. 2006;201;1.
57. Li XH, Deng SD, Fu H, Mu GN. Synthesis of thiazole based 1,3,4-oxadiazole derivatives and their corrosion inhibition characteristics at mild steel/hydrochloric acid interface. Corros. Sci. 2010;52:1167.
58. Li XH, Deng SD, Fu H, Mu GN. Synthesis of thiazole based 1,3,4-oxadiazole derivatives and their corrosion inhibition characteristics at mild steel/hydrochloric acid interface. Corros. Sci. 2008;50:2635.
59. Döner A, Kardas G. N-Aminorhodanine Investigation of corrosion inhibition effect of 3-[(2-hydroxy-benzylidene)-amino]-2-thioxo-thiazolidin-4-one on corrosion of mild steel in the acidic medium. Corros. Sci. 2011;53:4223.
60. Moretti G, Quartarone G, Tassan A, Zingales A, J. New synthesized 1,4-benzodiazine derivatives as corrosion inhibitors for mild steel in sulphuric acid, Werkst. Korros. 1994;45:641.
61. Ateya BG, El-Anadouli BE, El-Nizamv FM. Corros. Sci. 1984;24:509.
62. Assaf FH, Abou-Krish M, El-Shahawy AS, Makhoul MTh, Hala Soudy. Effects of Arctostaphylos uva-ursi Extract as Green Corrosion Inhibitor for Cu10Ni Alloy in 1 M HNO₃ Int. J. Electrochem. Sci. 2007;2:169.
63. Sekine I, Sabongi M, Hagiuda H, Oshibe T, Yuasa M, Imahc T, Shibata Y, Wake T. New Benzonitrile Azo Dyes as Corrosion Inhibitors for Carbon Steel in Hydrochloric Acid Solutions, J. Electrochem. Soc. 1992;139:3167.
64. Larabi L, Benali O, Mekelleche SM, Harek Y. Inhibiting effects of 2-mercapto-1-methylimidazole on copper corrosion in 0.5 M sulfuric acid. Journal of Saudi Chemical Society. 2006;253:1371.
65. Lagrenee M, Mernari B, Bouanis B, Traisnel M, Bentiss F. 1-Benzoyl-4-phenyl-3-thiosemicarbazide as Corrosion Inhibitor for Carbon Steel in H₃PO₄ Solution. Corros. Sci. 2002;44:573.
66. Caigman GA, Metcalf SK, Holt EM. Corrosion inhibition of copper in HNO₃ solution using thiophene and its derivatives. J. Chem. Cryst. 2000;30:415.
67. Ashish Kumar Singh, Quraishi MA. A Novel corrosion inhibitor for mild steel in acid media. Corros. Sci. 2010;52:15.

© 2015 Fouda et al.; This is an Open Access article distributed under the terms of the Creative Commons Attribution License (<http://creativecommons.org/licenses/by/4.0>), which permits unrestricted use, distribution, and reproduction in any medium, provided the original work is properly cited.

Peer-review history:

The peer review history for this paper can be accessed here:
<http://www.sciencedomain.org/review-history.php?iid=1050&id=7&aid=9303>